Available online at www.sciencedirect.com

ScienceDirect

journal homepage: http://www.elsevier.com/locate/acme

Original Research Article

Analysis of tube deformation process in a new pilger cold rolling process

D. Pociecha *, *B. Boryczko*, *J. Osika*, *M. Mroczkowski*

Department of Metal Working and Physical Metallurgy of Non-Ferrous Metals, Faculty of Non-Ferrous Metals, AGH University of Science and Technology, 30 Mickiewicza Av., 30-059 Krakow, Poland

ARTICLE INFO

Article history:
Received 20 November 2013
Accepted 1 January 2014
Available online 24 January 2014

Keywords:
Pilger rolling process
Physical modelling
Numerical simulation

ABSTRACT

The paper presents the results of an experiment and numerical simulation in a new pilger tube cold-rolling process, in which the rolling stand is stationary and the rolled tube is placed on a slide and between the rollers. The experiment was conducted in a laboratory pilger mill operating according to a new concept of rolling. Numerical simulations were performed with the registration of the entire history of deformation of the rolled tube. Despite a simplification in the mathematical modelling, the obtained results were very similar to the experiment results. Pilger rolling, carried out according to a new concept, can be successfully used for the industrial production of non-ferrous metal pipes. Pipes obtained after the rolling process are suitable for further processing or for direct sale. Particular attention, however, should be paid to ensure sufficient structural rigidity in the mill, as well as to the quality and accuracy of the tools used in the pilger process.

1. Introduction

Cold rolling of tubes in pilger mills is a cyclical process that is commonly used in manufacturing of tubes made of hardly deformable alloys. In the classic solution [1,2], the rolling stand is mobile and moves to-and-fro, and the rollers move with the stand, while turning in opposite directions. A circular groove is cut in the roller, so that in the entry plane, the groove cross-section is equal to the cross section of the blank feed tube, while in the exit plane it is equal to the cross section of a finished tube. The groove diameters are selected so that in extreme positions, in the stand, rollers do not contact the metal. Calculation of the shape and dimensions of rollers (Fig. 1) and the mandrel is called a tool calibration.

Optimal calibration should ensure minimal use of rollers, high quality of rolled tubes and high process efficiency. The authors of the calibration methods select the shape of generating lines so as to ensure a decreasing wall draft down to zero at the end of the rolling zone [3], or to ensure even distribution of pressure on the rout of the stand work and a minimum power consumption [4].

Analysis of the results of research conducted by the authors of papers [5,6] showed that the possibilities of intensifying the classic process have been exhausted. One cannot increase the unit limit deformation and process efficiency in the classical pilger rolling process.

New design for the pilger mill was proposed in [7]. The rolling stand is stationary and the rolled tube is placed on a slide and placed between the rollers (Fig. 2). The hydraulically driven slide is put into to-and-fro motion, and the rollers only rotate. In extreme slide positions, like in the classical process, the tube further rotated and the next step of rolling is applied. The above-described concept of the pilger milling process

* *Corresponding author*. Tel.: +48 126173337; fax: +48 126172632.
E-mail address: danpoc@agh.edu.pl (D. Pociecha).

1644-9665/$ – see front matter
http://dx.doi.org/10.1016/j.acme.2014.01.001

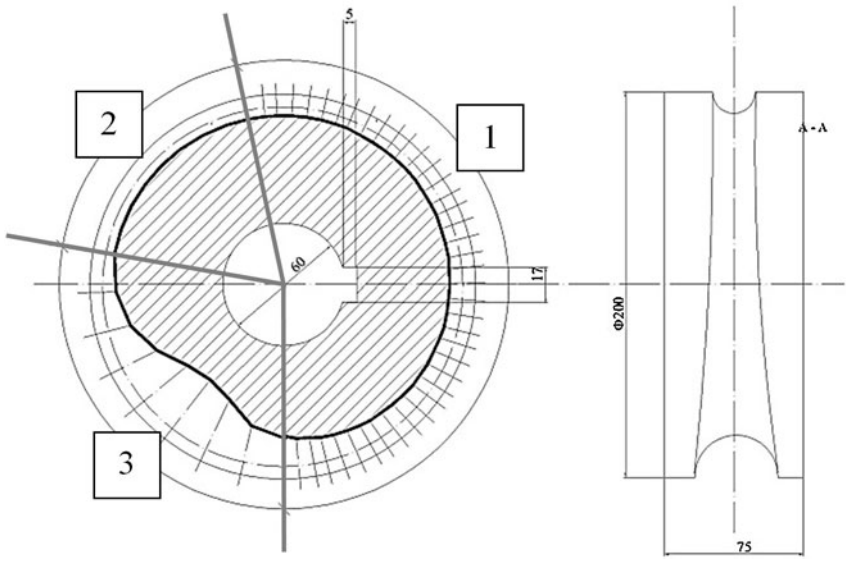

Fig. 1 – Roller calibration sample: (1) rolling zone, (2) calibration zone and (3) clearance.

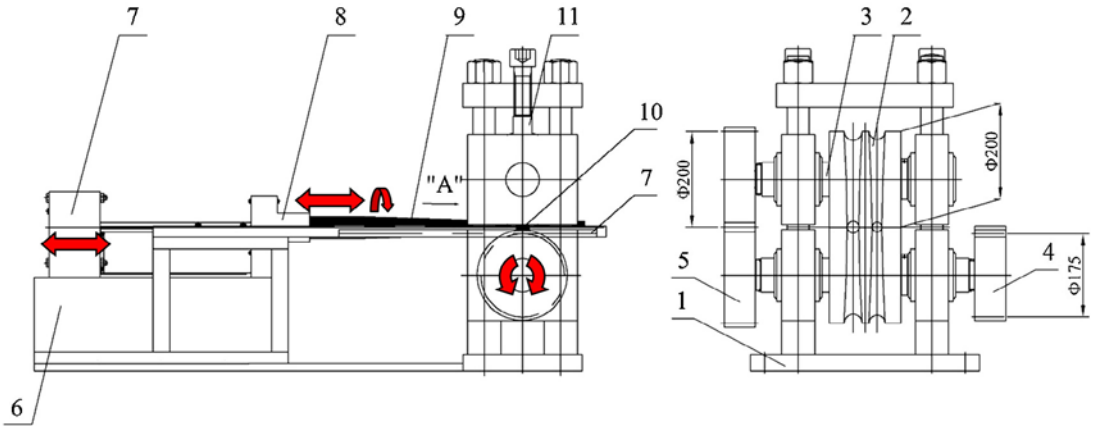

Fig. 2 – The new generation of the pilger rolling mill used for the physical modelling of the tube cold rolling: (1) rolling stand, (2) ring roll*, (3) work roll*, (4) gear wheel*, (5) transmission gear 1:1*, (6) slide base, (7) sliding and rotating mechanism, (8) initial tube carriage***, (9) tube***, (10) gear strip**, (11) pressure measurement system. Red arrows indicates movement and rotation. *Rotation, **to-and-fro movement, ***to-and-fro movement with tube rotation.**

became the basis for design of a new generation pilger mill. The advantages of the presented technical solutions include a reduction by more than a half of the weight of moving masses, may increase roller diameters, thus lengthening the working cone and practically unlimited increase of the stand stiffness.

In paper [7], the author states that the adoption of the new solution with a fixed stand and rollers only rotating changes the balance of forces transmitted from the drive to the stand, so one can expect a different state of stress in the working zone compared to the classical process. Confirmation of this thesis is modelling studies carried out in [8–10]. Further development and implementation of this technology requires knowledge of the impact of process parameters: on deformation of the rolled material and on pressure on rollers, and the preparation of a proper mathematical model of the process, which could in the future be used to optimize this technology. Due to the high degree of deformation occurring during the pilger process, the paper proposes a dedicated method for deformation measurement based on the principles of photogrammetry [11], together with software for a quick execution of calculations: Anot software enables an automatic annotation of measurements markers on tested tubes [12], and Fotogrant2008 is used to determine the spatial coordinates of makers [13,14].

Determination of deformation value is also possible with the use of numerical simulations. Numerical models of the classical pilger process are known from research carried out on zirconium tubes used in the nuclear industry. Models are based on one or three complete cycles of a working rolling stand. From the point of view of the model complexity and calculation time, this simplification is justified by the fact that a finished zirconium tube is obtained in 54 work cycles. Unfortunately, in this case, the deformation history of the rolled tube is not included, or is approximated on the basis of

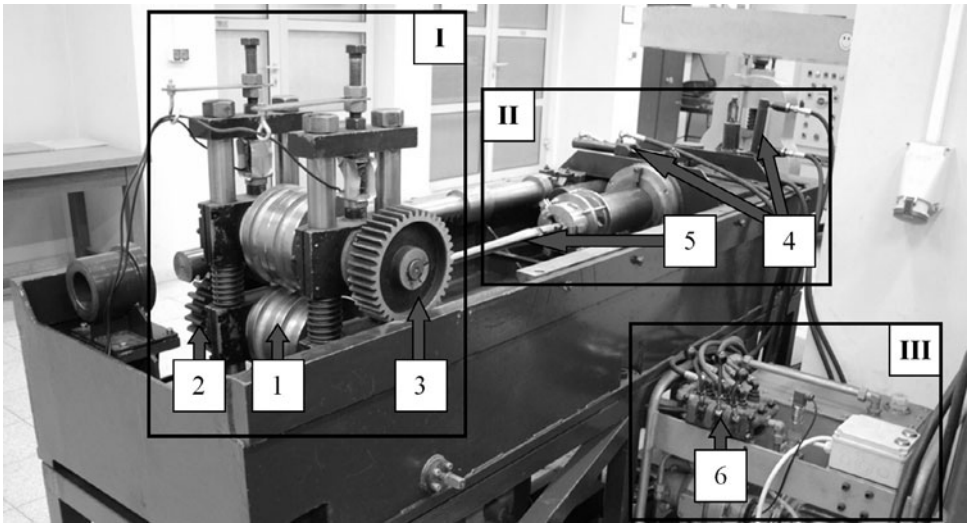

Fig. 3 – Laboratory pilger mill: (I) rolling stand, (II) sledge, (III) hydraulic drive, (1) rollers, (2) gear strip, (3) transmission gear 1:1, (4) tube feed and rotation mechanism, (5) mandrel, (6) shifters to control hydraulic actuators.

one cycle, which can cause significant errors in modelling [15–18].

2. Experiment

The experiment was conducted in a laboratory pilger mill according to a new concept shown in Fig. 3. Tools, i.e. the rollers and mandrel were made of tool steel.

Soft aluminium tubes were used as a batch. The tool shapes were designed based on the assumptions used for calibrating a classic pilger process [19]. The study adopted the following rolling program:

$$D_0 = 45.0 \times g_0 = 4.50 \rightarrow D_1 = 24.7 \times g_1 = 1.12 \quad (1)$$

where D_0 and D_1 are the tube diameters before and after rolling, g_0 and g_1 are tube thickness before and after rolling, and the final tube dimension is obtained after 18 rolling cycles.

To determine the distribution of deformations in the working zone containing the tested aluminium tube, a grid was applied on its outer surface, and then the displacement of individual points in the subsequent stages of rolling was observed. On the basis of the displacements, deformations in individual working cycles were calculated. Due to the cyclical nature of the pilger process and large the final material deformation, obtaining a permanent grid to be applied onto the surface is extremely difficult. Grid becomes illegible after only a few working cycles. Therefore, copper sticks driven in an aluminium tube were used for the measurement. Due to the fact that copper has a good contrast with aluminium, the sticks are visible at each rolling stage (Fig. 4). Correctly placed copper sticks do not affect the metal flow during deformation, but if they are too numerous, it may result in tube cracking in the final stage of rolling, so it is not possible to make a high-density grid.

Stick position measurement was made using a measurement system based on the principles of photogrammetry. The method comprises a simultaneous creation of image pairs, using two cameras with similar optical performance, placed away from each other at an assumed distance, the so-called base. Using these two images, it is possible to determine X, Y, Z coordinates of any measurement point of the object, by measuring background mapping coordinates of this point on the left and right image. The stand preparation includes the making of a test chart, and placing it into the zone where tube with measuring points is (Fig. 4).

Using Anot and Fotogrant2008 software, the spatial coordinates of the tested points before and after deformation were determined. Assuming that for a single rolling cycle, the assumption of flat cross-sections is permitted, the total deformation of the rolled tube was calculated directly from the formula:

$$\varepsilon = \ln \frac{S_0}{S_1} \quad (2)$$

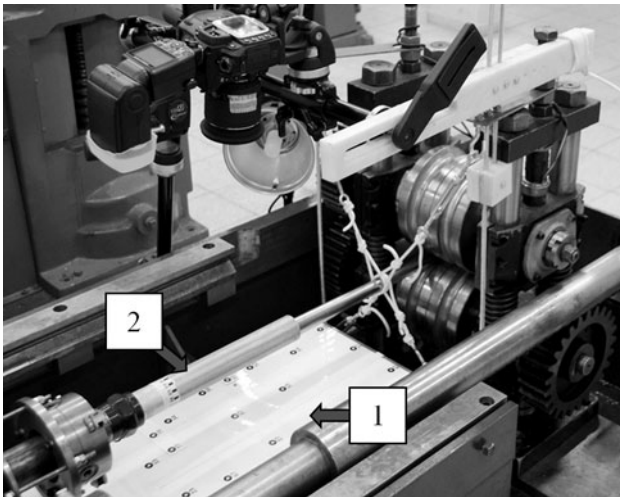

Fig. 4 – Laboratory pilger mill and measuring stand: (1) test chart and (2) tube with sticks.

where S_0 is the initial cross-section and S_1 is the final cross-section.

On the basis of the calculated deformation value dependencies were determined, depicting the actual deformation distribution along the working cone in a single rolling cycle, as well as the total deformation in the process.

During the rolling, the pressure of metal on the rollers was measured. A correct adoption of roll calibration should ensure an even distribution of forces across the cone work, and the value of metal pressure on rollers should not fall below 80% of the maximum rolling force:

$$F_{wmax} \geq F_{wdop} \geq 0.8 \cdot F_{wmax} \tag{3}$$

After rolling, the outer and inner surface of the tested tubes was assessed visually. Wall thickness distribution was measured, and E_c eccentricity and U relative wall thickness were determined. The collected results were compared before and after the rolling process. To determine the value of eccentricity and relative wall thickness, the following formula was used:

$$U = \frac{g_{max} - g_{min}}{g_{max} + g_{min}} \times 100\% \tag{4}$$

where g_{max} and g_{min}, the maximum and minimum thicknesses do not need to be measured at an angle of 180°

$$E_c = \frac{g_{max} - g_{min}}{g_{max} + g_{min}} \times 100\% \tag{5}$$

where g_{max} and g_{min} must be measured at an angle of 180°.

Thickness measurements were made using a non-destructive method, using a calibrated ultrasonic gauge.

3. Numerical simulation

Numerical simulations of the pilger process were performed using Abaqus software package. Mechanical properties of the material needed to build the model were determined based on the results of tensile tests. The coefficient of friction throughout the model – rollers/tube, tube/mandrel – was set at $\mu = 0.05$. A rolling program shown in (1) was adopted. A pilger process model is shown in Fig. 5.

The phenomena occurring during pilger rolling introduce a strong non-linearity of the model. These are primarily connecting with the cyclical nature of the process and complex contact problems. In order to simplify computing tasks, the following additional assumptions were made:

- Tools are recognized as infinitely rigid.
- During the deformation, no inertial force influences the rolled tube.
- The model does not take into account the effects of temperature and strain rate.

To solve the task, the explicit numerical method was used, characterized in that the calculation results are obtained by explicit integration method. Throughout the model, density scaling was applied, which made it possible to significantly reduce the time of the calculations. Time calculation for one model and eight-processor system did not exceed a week.

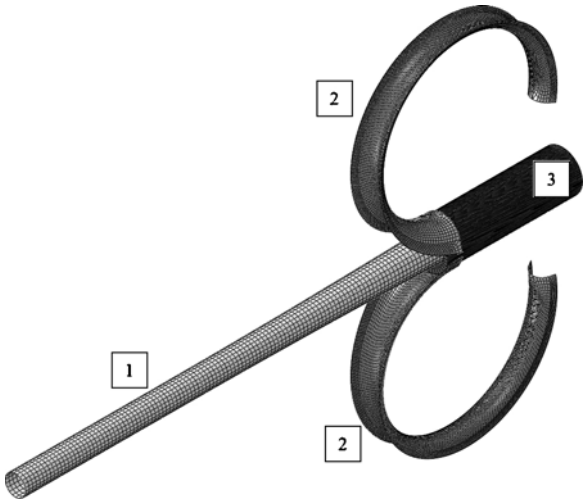

Fig. 5 – Numerical model of the pilger rolling process: (1) mandrel, (2) rollers and (3) tube.

Despite large deformations of the material, no mesh regenerating algorithms or optimization methods were used.

4. Results and discussion

Fig. 6 shows the results of a numerical simulation, showing the obtained plastic strain distributions in the rolled tube after 16 rolling cycles. On the tube longitudinal-section (Fig. 6a), it can be seen that the material flows almost uniformly. There were no overlaps, or large local deformation values. Visible small local strain gradients occur because the tube is rotated during the rolling process. It can be seen also that metal flows more intensively at the contact surface between tube and rolls (Fig. 6c). It is related to friction on the contact surface between the tube and mandrel (Fig. 6d).

In experimental studies, the effect of advance value feed on the deformation distribution along the length of the working cone was assessed (Fig. 7). For small advances, at 1 mm and 2 mm no a large impact on the deformation values was observed, only its further increase causes them to be quite significant. Due to the design of the hydraulic drive, the largest mill advance rate was 8 mm per cycle. In the early rolling stages, the material is hardly deformed at all, and for small advance values, one can also observe negative deformation values, which implies material upsetting. This is due to the fact that at the beginning, the tube does not come in contact with the mandrel from the inside, and it only changes its dimensions, i.e. the outer and inner diameter (Fig. 6d). Only at the moment of contact between the tube and mandrel does a very strong increase in deformation occur. The deformation value increases in the roller working zone, and then decreases prior to the entry of the material into the calibration zone. In the calibration zone, the material is not deformed strongly anymore; it is only that the final shape of the rolled tube is performed. For comparison, Fig. 7b shows the results of a numerical simulation of deformation in a single cycle, the advance rate being 8 mm. The results of both measurements physical and simulation cannot be compared directly – in the

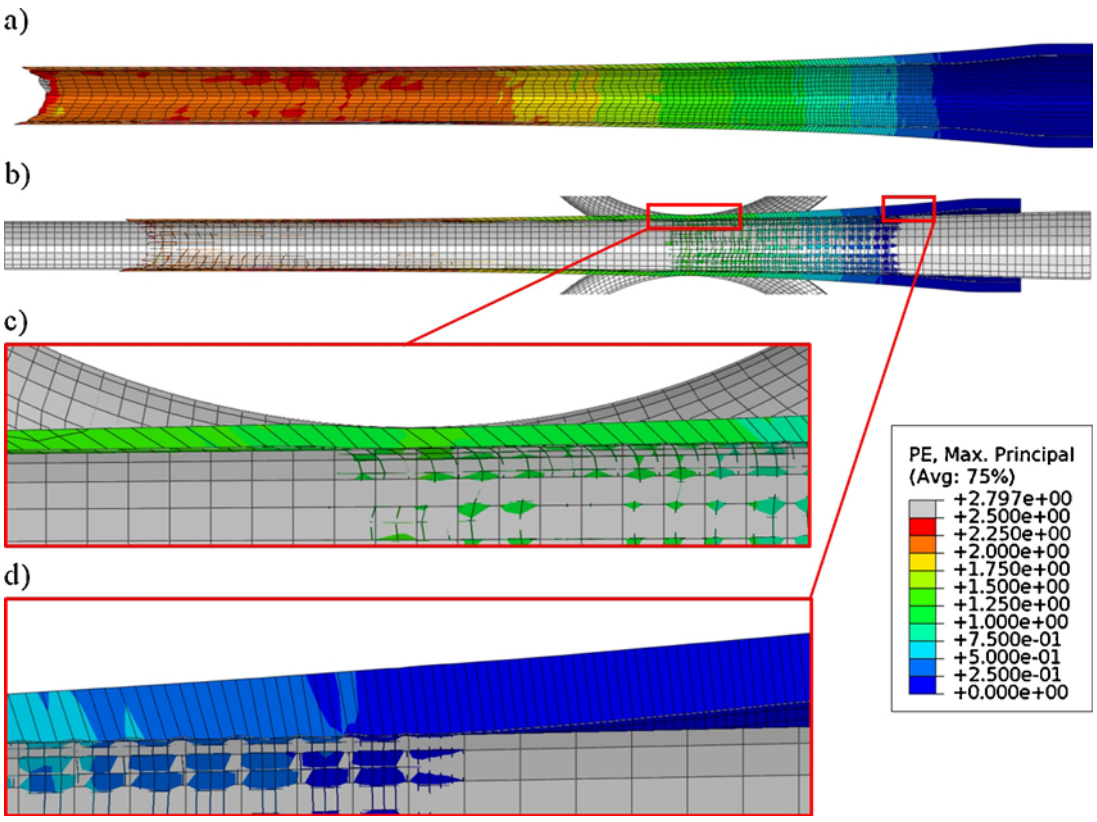

Fig. 6 – Longitudinal-section of the deformed tube: (a) grid after deformation, (b) working cone during the rolling process, (c) momentary working zone, (d) beginning of the contact material with mandrel. PE – plastic strain, tensor.

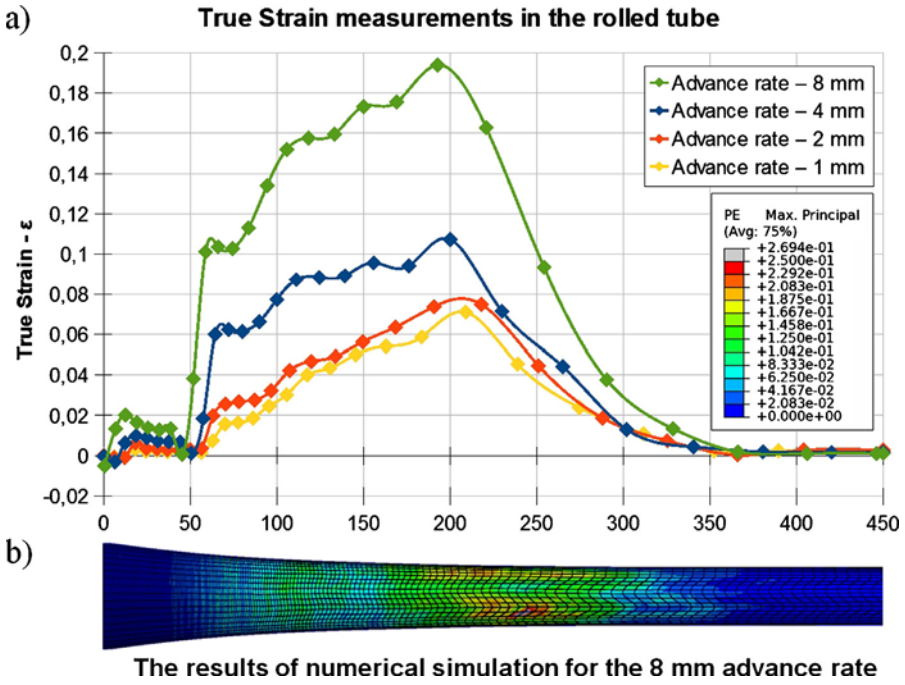

Fig. 7 – Strains distribution along the length of the working in the single cycle: (a) physical modelling and (b) numerical simulation.

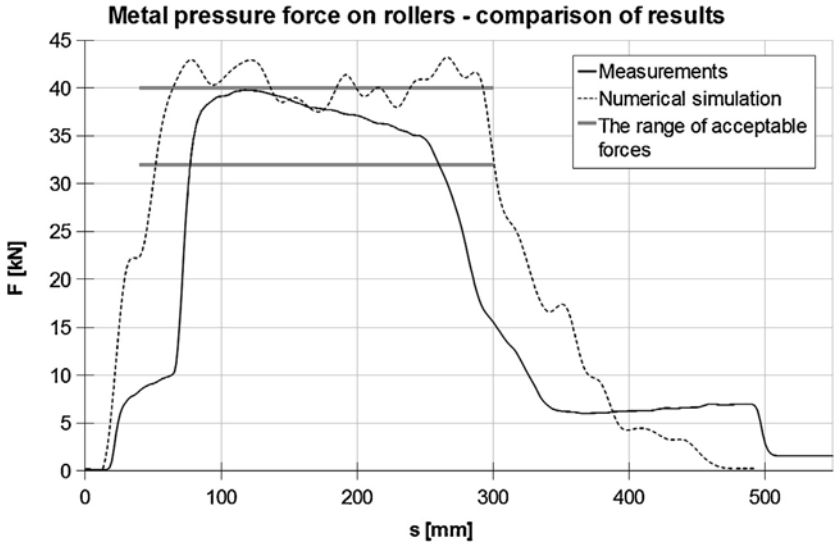

Fig. 8 – Metal pressure force on rollers for 8 mm advance rate, measurements and numerical simulation.

Fig. 9 – Aluminium tube after rolling process.

Table 1 – Eccentricity and relative wall thickness of tubes.

	Feed tube		Finished tube	
	Measurement	Standard deviation	Measurement	Standard deviation
U_{max}	9.85	0.05	6.36	0.76
Ec_{max}	9.28	0.11	4.90	0.58

physical model, the deformations are averaged for each pipe cross-section – it can be seen, however, that the deformation obtained from the numerical simulation and experiment are consistent.

Measurement of metal pressure force on rollers (measured in columns of mill stands) confirmed the results of the numerical simulation and the proper performance of the tool calibration. The pressure of metal exerted on rollers in the metal deformation zone along the working cone length is within the permissible limits (Fig. 8). It is worth noting that the graphs showing metal pressure force on rollers as shown in Fig. 8 do not overlap perfectly. The visible discrepancy is related to the accepted model simplifications that accumulate from cycle to cycle. Fig. 8 shows the forces when the metal has completely filled the working zone in the 18th cycle of rolling.

The last stage of the study included the determination of eccentricity and relative wall thickness after the tube rolling process. The test batches were extruded tubes with high eccentricity and relative wall thickness, and with uneven thickness distribution along the tube length. After rolling, a much more uniform thickness distribution was obtained, as well as and a lower tube eccentricity and relative wall thickness (Table 1).

Tubes were subjected to a visual inspection of the surface quality. The tube outer and inner surfaces are smooth and shiny (Fig. 9). There were no cracks or discontinuities in the flow of metal even with large values of the material advance.

5. Conclusions

The application of sticks to mark measurement points and of the photogrammetric method allowed the determination of deformation distribution in the process of cold pilger tube rolling. Despite the limitations associated with the grid density, the stick method is the only possible one to use,

due to the durability of measurement point marking, and the opportunity to observe the metal flow on the tube cross-section and longitudinal-section. The results showed that Anot and Fotogrant2008 software was very useful in this type of measurements, allowing the performance of fast and accurate calculations.

The created numerical model can be used to simulate the pilger rolling process. Despite the adoption of simplifications in the mathematical modelling, the results obtained were very similar to the results from the experiment.

Pilger rolling conducted according to the new concept can successfully be used for the industrial production of non-ferrous metal tubes. Tubes obtained after the rolling process are suitable for further processing or for direct sale. Particular attention, however, should be paid in order to ensure sufficient structural rigidity of the mill, and quality and accuracy of the tools prepared to carry out the pilger process.

The study allowed an analysis of a new pilger process for the adopted rolling program; Future research will be conducted in terms of refinement of the numerical model and the use of other metals such as copper or brass.

Funding

Work financed from statutory funds. Contract number: 11.11.180.655.

REFERENCES

[1] M. Baensch, New generation of cold pilger mills with higher productivity, low investment and maintenance costs, in: Tube Drawing & Extrusion Conference, April 1–3, Red Lion's La Posada Resort Scottsdale, Arizona, 1996.
[2] J. Osika, Walcowanie rur na zimno w walcarkach pielgrzymowych, AGH Uczelniane wydawnictwa naukowo-dydaktyczne, Kraków, 2004.
[3] P.K. Tietierin, Racjonalnaja kalibrovka walkov stanov cholodnoj prokatki trub, Stal, nr 12, 1953.
[4] J.F. ?evakin, Kalibrovka i usilja pri cholodnoj prokatke trub, Metallurgizdat, Moskva, 1963.
[5] M. Monkawa, S. Ueda, K. Kojima, M. Furugen, Stress analysis on the roll and mandrel of a cold pilger mill, Journal of Mechanical Working Technology 10 (1984) 351–358.
[6] J. Osika, K. Świątkowski, An investigations of displacement and deformation during cold rolling of tubes in pilgering process, in: 7th ICTP, October 27–November 1, Yokohama, Japan, 2002.
[7] J. Osika, Nowa koncepcja procesu walcowania rur na zimno w walcarkach pielgrzymowych, Rudy i Metale Nieżelazne 11 (2006) 629–634.
[8] J. Osika, H. Palkowski, K. Świątkowski, D. Pociecha, A. Kula, Analysis of material deformation during the new cold tube rolling process realized on the new generation of pilger mills, Archives of Metallurgy and Materials. Polish Academy of Sciences. Committee of Metallurgy. Institute of Metallurgy and Materials Science 54 (4) (2009) 1239–1251, ISSN: 1733-3490.
[9] H. Palkowski, D. Pociecha, J. Osika, K. Świątkowski, Wyznaczanie pól odkształceń w procesie walcowania pielgrzymowego rur miedzianych i aluminiowych, Rudy i Metale Nieżelazne 55 (11) (2010) 770–775, ISSN: 0035-9696.
[10] D. Pociecha, J. Osika, K. Świątkowski, H. Palkowski, Zastosowanie modelowania fizycznego do wyznaczania pola odkształceń w procesie pielgrzymowego walcowania rur na zimno, Polska Metalurgia w latach 2006–2010, 2010, 505–514, ISBN: 978-83-60958-64-3.
[11] J. Osika, D. Pociecha, M. Piwowarska, Stereofotogrametryczna metoda wyznaczania pól przemieszczeń w walcowaniu pielgrzymowym rur na zimno, Rudy i Metale Nieżelazne 55 (3) (2010) 137–142, ISSN: 0035-9696.
[12] D. Pociecha, J. Osika, M. Mroczkowski, B. Boryczko, Prototypowy system pomiaru odkształceń w procesie walcowania pielgrzymowego rur na zimno, Mechanika 253 (2013) 25–30, ISSN: 0137-2335. Bibliogr. s. 30. – ISBN: 978-83-7814-098-6.
[13] D. Pociecha, M. Jabłoński, Stanowisko wizyjnego śledzenia odkształceń metalu w procesie obróbki plastycznej na zimno, Automatyka: półrocznik Akademii Górniczo-Hutniczej im. Stanisława Staszica w Krakowie 14 (3/1) (2010) 453–465, ISSN: 1429-3447.
[14] M. Jabłoński, D. Pociecha, Automatyczna anotacja znaczników sztyftowych w procesie walcowania pielgrzymowego rur na zimno, Automatyka: półrocznik Akademii Górniczo-Hutniczej im. Stanisława Staszica w Krakowie 14 (3/1) (2010) 289–299, ISSN: 1429-3447.
[15] S. Mulot, A. Hacquin, P. Montmitonnet, J.-L. Aubin, A fully 3D finite element simulation of cold pilgering, Journal of Materials Processing Technology 60 (June (1–4)) (1996) 505–512.
[16] P. Montmitonnet, R. Logé, M. Hamery, Y. Chastel, J.-L. Doudoux, J.-L. Aubin, 3D elastic–plastic finite element simulation of cold pilgering of zircaloy tubes, Journal of Materials Processing Technology 125–126 (September) (2002) 814–820.
[17] B. Lodej, K. Niang, P. Montmitonnet, J.-L. Aubin, Accelerated 3D FEM computation of the mechanical history of the metal deformation in cold pilgering of tubes, Journal of Materials Processing Technology 177 (2006) 188–191.
[18] M. Harada, A. Honda, S. Toyoshima, Simulation of Cold Pilgering Process by a Generalize Plane Strain FEM, ASTM Special Technical Publication, 2006pp. 233–247 NUMB 1467.
[19] J. Bazan, J. Osika, Metoda zespolonego kalibrowania narzędzi do walcowania rur na zimno na walcarkach pielgrzymowych, Zeszyty Naukowe AGH, Metalurgia i Odlewnictwo 438 (1974) 225–244.